September/October 1999 · Vol. 1 · No. 6

Molecular refinement of karyotype: Beyond the cytogenetic band

D. Alexa Sirko-Osadsa, PhD, Suzanne B. Cassidy, MD, Theresa W. Depinet, BS, Nathaniel H. Robin, MD, Chanin Limwongse, MD, Stuart Schwartz, PhD

Purpose: Illustrate the use of molecular methodologies to delineate subtle, de novo, chromosome aberrations and determine the presence, or absence, of known genes, allowing improved predictions of long-term phenotypic effect. **Method:** High-resolution chromosome analysis followed by FISH and microsatellite analysis to determine the extent and parental origin of the abnormalities. **Results:** Four de novo deletions involving chromosomes 5q, 10q, and 16p were delineated molecularly. Specific genes were shown to be, or not to be, involved in each aberration, refining karyotype-genotype correlation. **Conclusion:** Molecular characterization of subtle chromosomal aberrations can provide information to assist in predicting clinical outcome in cases involving genes known to have an effect due to haploinsufficiency or aberrant gene dosage. ***Genetics in Medicine*, 1999:1(6):254–261.**

Key Words: *molecular cytogenetics, FISH, microsatellites, deletions*

Molecular cytogenetic techniques have advanced to allow the characterization and delineation of subtle, cytogenetically detected chromosome aberrations, such as deletions and duplications. While high-resolution chromosome analysis can serve to provide the initial detection and cytogenetic localization of a de novo chromosomal abnormality, this method is limited in sensitivity to what can be visualized under the microscope and, therefore, does not necessarily provide sufficient information to allow a prediction of phenotype or natural history. This initial cytogenetic information can be augmented by molecular analysis, which will furnish additional data to allow the extent of the abnormality to be better defined. Delineation at the molecular level is essential to verify the presence or absence of specific genes included within a chromosomal abnormality.

This approach can provide the means for making predictions about the long-term phenotypic effect engendered by aberrant gene dosage due to the duplication of a particular locus, or to its haploinsufficiency through deletion. The ability to make such predictions has evolved from the integration of clinical, cytogenetic, and molecular data garnered from the study of individuals harboring simple deletions or duplications. Deletion analysis has been used extensively to correlate phenotypic effects with monosomy for specific chromosomal bands and provide information that has allowed numerous genes to be specifically localized.

From the Department of Genetics and Center for Human Genetics, Case Western Reserve University School of Medicine and University Hospitals of Cleveland, Cleveland, Ohio.

Stuart Schwartz, PhD, Center for Human Genetics Laboratory, 10524 Euclid Avenue, 6th Floor, Cleveland, OH 44106-9959.

Received June 11, 1999.

Accepted August 23, 1999.

In a classical example, the localization of the retinoblastoma gene *RB1*, and its eventual assignment to chromosome 13q14,[1] evolved from the initial observation that a D group chromosome was partially deleted in retinoblastoma tumor tissue[2] and continued with reports of retinoblastoma in patients harboring a constitutional deletion in the long arm of a D group chromosome.[3,4] The identification of gene mutations in Familial Adenomatous Polyposis emanated from the study of a patient with a constitutional interstitial deletion of 5q and a presumed contiguous gene syndrome that included multiple adenomatous polyposis of the colon.[5] Molecular analysis of patients with Rubinstein-Taybi syndrome, a chromosome 16p13.3 microdeletion syndrome, associated the pathology of this syndrome with a single gene encoding the transcriptional coactivator CREB binding protein.[6]

In combination with the profusion of genomic data attributable to the efforts of the Human Genome Project, such studies have led to the localization of an increasing number of genes and to making significant correlations between haploinsufficiency for a discrete genetic locus and a particular phenotype. Such associations, in combination with molecular cytogenetic analysis, provide the means for allowing karyotype-phenotype corellations to be made for patients with de novo chromosome aberrations.

The objective of our ongoing studies is to use molecular methodologies to delineate subtle, de novo chromosome aberrations to determine the presence or absence of known genes in the associated regions. We report the results of the cytogenetic, molecular, and molecular cytogenetic analyses of four small, de novo deletions to determine if known genes, with quantitative phenotypic effects, were involved. Two of the cases involved deletions in chromosome 5q; one case had a deletion in 10q that will be compared to a case previously reported by our group; and one had a deletion of distal 16p. These studies have

allowed us to make better predictions of phenotype, inasmuch as refined phenotype-genotype correlations were made subsequent to the initial identification of the cytogenetic abnormalities.

MATERIALS AND METHODS

Subjects

Patient 1 was a male with a history of atrial septal defect, pulmonary stenosis, mild to moderate growth retardation, and global developmental delay. He was the full-term product of an uncomplicated G_1P_0 pregnancy in a 21-year-old mother, but had difficulty in the neonatal period due to his congenital cardiac problems. Clinical genetics evaluation at 3 years of age revealed him to have bilateral epicanthal folds, a flat nasal bridge, anteverted nares, mild joint laxity, mild truncal hypotonia, and cryptorchidism. Ophthalmologic evaluation identified congenital hyperplasia of retinal pigmented epithelium (CHRPE). His height and weight were below the 5th percentile.

Patient 2 was a male referred for genetics evaluation due to speech delay. He was the 39-week product of an uncomplicated pregnancy in a 34-year-old G_2P_1 woman. With the exception of his delayed language development and delayed attention span, he was developmentally normal. His height was just above the 50th percentile and his weight between the 90th and 97th percentiles. His physical exam at age 17 months was unremarkable except for a mildly high arched palate and a superiorly overfolded left auricle helix.

Patient 3 was a male born at 36 weeks gestation after an uncomplicated pregnancy in a 37-year-old G_1P_0 mother. His history was remarkable for a two-vessel cord, sacral dimple, and right clubfoot noted at birth, and he had transient tachypnea of the newborn and transient hyperbilirubinemia. At 2 months of age, he was diagnosed with bilateral inguinal and umbilical hernias, which were surgically repaired. At 12 months, he was diagnosed with a small VSD, which spontaneously closed by 4 years of age, and bilateral exotropia, which was surgically repaired. He had generalized ligamentous laxity beginning early in life. A clinical genetics evaluation at 5 years of age revealed normal growth and development. His head circumference was normal, and his cranium symmetrical, with a slightly prominent forehead. He had mildly up-slanting palpebral fissures, and interpupillary distance at the 97th percentile. His nose was normal, but he had mid-face hypoplasia, malar flattening, and a flat facial profile. His palate was high and asymmetric, and he had an underbite. His ears were normally shaped and normally placed. His genitalia were normal, and his anus normally placed. He had hyperextensible hand joints, normal palmar creases, and soft and velvety skin.

Patient 4 was a girl with a history of right hip dysplasia, congenital lumbar scoliosis and mild developmental delay. She was the 35-week product of the uncomplicated pregnancy in a G_1P_0 mother. Her birth weight was at the 50th percentile and her length was between the 10th and 25th percentiles. A clinical genetics evaluation at 15 months of age showed her height to be at the 15th percentile, and her weight at the 25th percentile. Plagiocephaly, a single posterior hair whorl, and low posterior hairline were noted, as was hypertelorism and a low-set, slightly cupped, right ear. She had a flat nasal tip with a midline nasal raphe and a smooth upper vermilion border. There was slightly redundant skin on her posterior neck, and her chest was broad, with widely spaced nipples.

There was no known consanguinity in any of the families, and no family history of mental retardation, putative genetic disorders, or other birth defects.

Cytogenetic analysis

High-resolution analysis of GTG-banded chromosomes (600–750 bands) from peripheral blood was performed as described elsewhere.[7] Briefly, PHA-stimulated blood leukocytes were cultured for approximately 72 hours in RPMI 1640 with 17% fetal bovine serum. Cultures were synchronized by addition of thymidine for the last 16.5 hours of culture and harvested after addition of ethidium bromide and colcemid for the last 45 minutes and 25 minutes of culture, respectively. Cells were treated with 75 mM KCl for 8 minutes and fixed in 3:1 methanol:acetic acid before staining.

Microsatellite analysis

When parental bloods were available, the extent and parental origin of the deletions were determined using panels of highly polymorphic microsatellite repeat markers (MapPairs, Research Genetics, Huntsville, AL) in the appropriate regions. Markers were selected using information from the integrated genetic, physical, and cytogenetic maps of the Genome Database (GDB), Johns Hopkins University,[8] the Genetic Location Database (LDB), University of Southampton, Wessex Human Genetics Institute;[9] and the NCBI UniGene human sequences collection.[10]

Genomic DNA was extracted from peripheral blood using standard techniques with the PureGene DNA isolation kit (Gentra Systems, Minneapolis, MN). One hundred to 200 ng of purified genomic DNA was used as template for PCR analysis of microsatellite markers according to the method of Micale et al.[11]

Fluorescence in situ hybridization

Fluorescence in situ hybridization (FISH) was employed to determine the extent of the deletions when parental bloods were not available, or to provide initial characterization before microsatellite analysis. Hybridizations were performed on metaphase cells using the methodology of Pinkel et al.[12] with minor modifications.[13] Yeast artificial chromosome (YAC) clones (Research Genetics, Huntsville, AL), P1 clones (Genome Systems, St. Louis, MO), and cosmids used in FISH analysis were selected from the vicinity of the patients' deletion breakpoints using information from the integrated genetic, physical, and cytogenetic maps of the Whitehead Institute database.[14]

The YACs were biotin-labeled by nick translation (Gibco-BRL, Gaithersburg, MD), and denatured probe mixture (labeled probe in 55% formamide, 10% dextran sulfate, 0.5

mg/mL herring testes DNA, and 2 × SSC) was applied to slides denatured in 70% formamide at 70°C. Hybridization was performed overnight at 37°C. Slides were washed in 50% formamide per 2 × SSC at 43°C for 15 minutes, followed by a 2 × SSC wash at 37°C for 8 minutes. Signal was detected by the avidin-fluorescein isothiocyanate amplification method.[12] For each probe, at least 20 metaphase cells were analyzed. Digital images were captured using a Zeiss epifluorescence microscope equipped with a cooled CCD camera (Photometrics CH250) controlled by an Apple Macintosh computer.

The physical length of each deletion was estimated by calculating the radiation hybrid map (Genebridge 4 panel) distance between the two markers flanking the deletion using the kilobase per centiray equivalent defined for each chromosome.[15]

RESULTS

Patient 1

High-resolution cytogenetic analysis of peripheral blood leukocytes from Patient 1 revealed a 46,XY,del5(q15q22) karyotype; both parents were found to have normal karyotypes. The adenomatous polyposis coli (APC) (MIM 175100) gene, *APC*, associated with the development of colon polyps and an increased risk for colon cancer[16] is mapped to 5q21-q23,[17] thus it was possible that *APC* was included in the deletion. Accordingly, the molecular characterization of this deletion first sought to determine if *APC* was present or absent, and second, to delineate the extent and parental origin of the deletion. We initially analyzed two microsatellite markers tightly linked to *APC*, D5S346 and D5S82,[18] and with both markers the paternal allele was absent, suggesting a deletion of this gene (Fig. 1). To determine the size of the deletion, nine additional markers extending both proximally and distally from D5S346 and D5S82 were analyzed. Five of these additional markers demonstrated deletion of the paternal alleles; three showed a biparental inheritance pattern; and one was uninformative (Table 1). The proximal breakpoint was localized to the area between markers D5S433 and D5S492 in band 5q21, while the distal breakpoint was found to lie between D5S2098 and D5S2110 in band 5q23. Based on radiation hybrid physical mapping data, the estimated size of the deletion in this patient is approximately 8 Mb.

Patient 2

High-resolution chromosome analysis of peripheral blood leukocytes from this patient revealed a 46,XY,del(5)(q14.1q21.1) karyotype; both parents were found to be cytogenetically normal. By cytogenetic analysis, the deletion in this patient appeared to overlap that of Patient 1 and, similarly, suggested the possible involvement of the APC gene. Analysis of *APC* markers D5S82 and D5S346 demonstrated biparental inheritance; therefore, in view of the cytogenetic findings, we continued our study by testing markers located proximal to this region (Table 1). Nine additional microsatellite markers were analyzed, and eight were informative. Four of these markers demonstrated biparental inheritance, and four revealed the deletion of paternal alleles. The deletion was found to extend from a region between marker D5S433 in 5q23.1 and D5S495, in 5q21.1 to an area between markers D5S652 and D5S618 in 5q14.1, suggesting the loss of approximately 7 Mb (Fig. 1). Thus, this deletion was found not to overlap that of Patient 1 and not to include *APC*.

Patient 3

High-resolution chromosome analysis of peripheral blood leukocytes from Patient 3 revealed a 46,XY,del(10)(q22.3q23.2) karyotype.

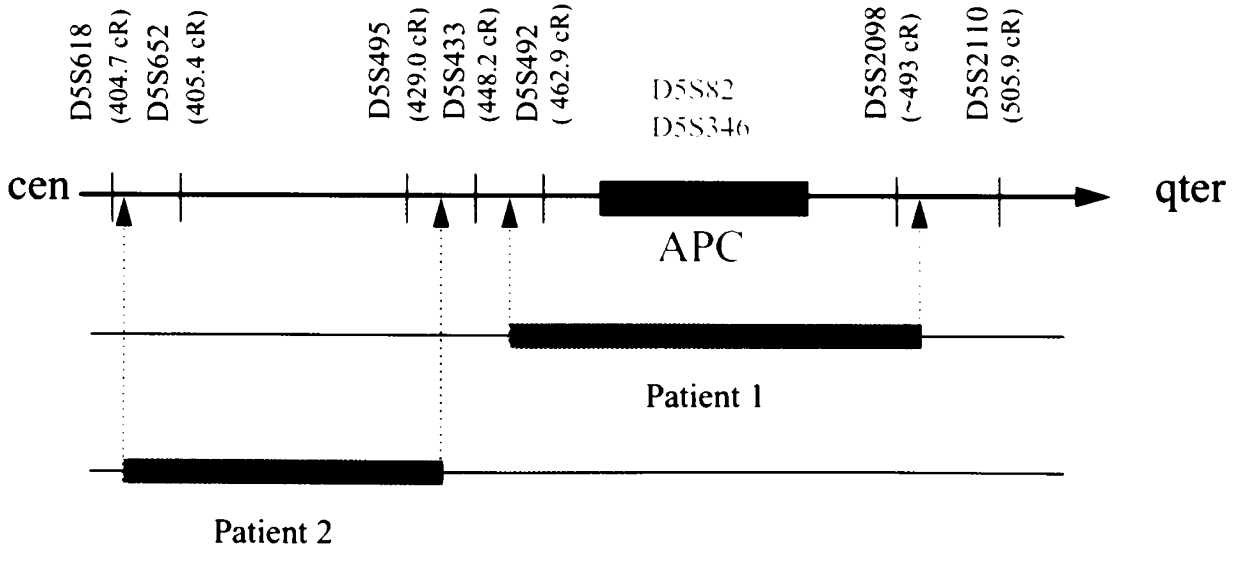

Fig. 1 Diagrammatic representation of chromosome 5q, not drawn to scale, denoting the regions deleted in patients 1 and 2. The long arm of chromosome 5 is depicted by the black arrow, and representative microsatellite markers, arrayed by physical location in centiRays (cR), are shown above. For each patient, a black bar identifies the deleted region, with the approximate breakpoints indicated by the dotted lines. Patient 1 demonstrates a deletion that includes the *APC* region, while the deletion in patient 2 does not include *APC*. The order of the markers and physical mapping information, in cR3000 units, are from the databases indicated in the text. For chromosome 5, the physical to genetic map correlate is 1 cR = 272 kb (Gyapay et al.).[15]

Table 1
Chromosome 5 microsatellite analysis of patients 1 and 2

Microsatellite	Physical distance (cR) 1 cR = 272 kb	Inheritance pattern	
		Patient 1	Patient 2
D5S401	402.92		biparental
D5S618	404.74		biparental
D5S652	405.41		paternal allele deleted
D5S644	419.8		paternal allele deleted
D5S484	423.5		paternal allele deleted
D5S495	429.02		paternal allele deleted
D5S409	437.03		uninformative
D5S433	448.17	biparental	biparental
D5S492	462.95	paternal allele deleted	biparental
D5S82	463–472	paternal allele deleted	biparental
D5S346	463–472	paternal allele deleted	biparental
D5S1965	463–472	uninformative	
D5S421	463–472	paternal allele deleted	
D5S404	472–476	paternal allele deleted	
D5S1975	491–486	paternal allele deleted	
D5S2098	491–496	paternal allele deleted	
D5S2110	505.9	biparental inheritance	
D5S500	522.4	biparental inheritance	

Both parents were found to have normal karyotypes. The tumor suppressor gene, *PTEN*, associated with Cowden disease (MIM 158350) and Bannayan-Riley-Ruvalcaba syndrome (MIM 153480), is mapped to chromosome 10q23.[19] Because cytogenetic analysis showed that the deletion extended to band 10q23.2, we sought to determine if *PTEN* was involved. FISH studies were initiated by hybridization with YAC 738B12, which includes the *PTEN* region. A signal was observed on the long arm of each of the chromosome 10 homologues, as was the case with hybridization using YAC 944E1, located telomeric to this region. Further analysis with YACs 920H4 and 898C3, located centromeric to the *PTEN* region, each showed a signal on the 10q arm of the normal chromosome only (Fig. 2). Thus, the deletion in this patient was localized proximal to the *PTEN* region. Based on the genetic mapping information for microsatellites contained within the YACs used in this analysis, the distal breakpoint of the deletion is estimated to be at least 1.5 Mb proximal to *PTEN* (Fig. 3).

Patient 4

High-resolution chromosome analysis of peripheral blood leukocytes from this patient revealed a 46,XX,del(16)(p13.3p13.3) karyotype. Both parents were found to have normal karyotypes. Several important genes with defined phenotypic consequences map to chromosome 16p13.3. Included among these is the gene, *CBP*, encoding the CREB binding protein, the deletion of which is associated with Rubinstein-Taybi syndrome (MIM 18,0849); and *PKD1*, associated with polycystic kidney disease type 1 (PKD1) (MIM 601313). Also in this region is the tuberin gene, *TSC2*, associated with tuberous sclerosis (TSC) (MIM 191092); and the α-globin gene cluster, associated with α-thalassemia (MIM 141800). Hybridization with a whole chromosome 16 library painted the entire abnormal chromosome, indicating that the composition of the abnormal chromosome was specific to chromosome 16. Molecular analysis was initiated from the proximal end of band 16p13.3 to localize the breakpoint of this apparently terminal deletion. Hybridization of cosmid RT100 (a generous gift from Dr. Fred Petrij), specific to *CBP*, demonstrated signals on both chromosome 16 homologues, as did hybridization of the P1 clone 3699 (a generous gift from Dr. Arun Kumar), which is specific to *TSC2*. Thus, neither of these genes was deleted in this patient. *PKD1* is located immediately adjacent to the *TSC2* locus in a genomic region that is reiterated more proximally on 16p.[20] Thus, the presence of *PKD1* on both chromosome 16 homologues in this patient can be inferred by the presence of the flanking genes, *TSC2* and *CBP*.

De novo deletion of the most distal region of 16p13.3, which contains the α-globin genes, is associated with the α-thalassemia/mental retardation syndrome, ATR-16 (MIM 141750). The ATR-16 critical region is localized to the area between microsatellite markers D16S521 and D16S83, and includes approximately 2 Mb.[21] Two YACs within this region, 650A8 and 825H12, each demonstrated a signal only on the normal chromosome 16 homologue in this patient (Fig. 2). Thus, this patient's deletion appeared to include the ATR-16 critical region. To determine if the entire critical region was deleted, we analyzed microsatellite D16S3024, located approximately 7 Mb from 16pter, which revealed deletion of the paternal allele. Thus, this patient was determined to have a deletion that extends at least 7 Mb and includes the entire ATR-16 critical region, suggesting α-thalassemia/mental retardation syndrome, while loci for tuberous sclerosis, polycystic kidney disease, and Rubinstein-Taybi were not deleted (Fig. 4).

DISCUSSION

We have used molecular cytogenetic methodologies to delineate and, therefore, define the physical size of the regions involved in four de novo deletions detected by high-resolution chromosome analysis. Because in each case the deletions were found to be in areas that include known genes with defined

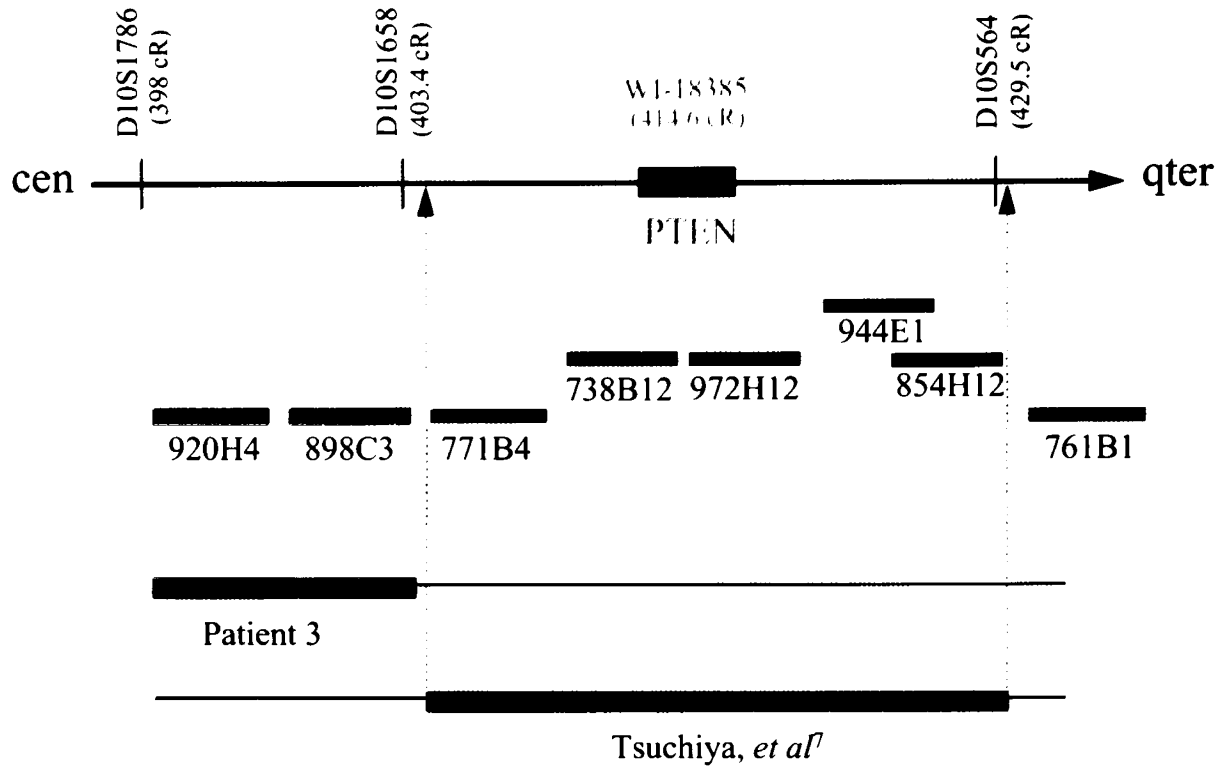

Fig. 2 Diagrammatic representation of chromosome 10q, not drawn to scale, denoting the deletion breakpoint in Patient 3 The long arm of chromosome 10 is depicted by the black arrow. YACs hybridized to the chromosomes of both Patient 3 and the patient of Tsuchiya et al.[7] are shown below. A black bar identifies the deleted region, with the approximate breakpoint indicated by the dotted line. The relative positions of the YACs are demonstrated using physical mapping distances between the STSs shown above. YAC 738B12, which includes the *PTEN* region, and YAC 944E1, located telomeric to *PTEN*, were not deleted in this patient. Further analysis with YACs 920H4 and 898C3, located centromeric to the *PTEN* region, each showed a signal on the 10q arm of the normal chromosome only.

phenotypic effects, we endeavored to determine the presence or absence of these known genes for each deletion, to make some predictions of long-term outcome.

By cytogenetic analysis, the 5q deletions identified in patients 1 and 2 appeared to overlap. However, molecular delineation of these deletions demonstrated that, while Patient 1 was deleted for *APC*, Patient 2 was not. Extension of our analysis to the regions flanking *APC*, and to the areas predicted by cytogenetic analysis to contain the breakpoints, further revealed that the deletions, although initially thought to overlap, were molecularly distinct, as neither patient was deleted for the microsatellite marker D5S654. In fact, the deletions were separated by at least 4 Mb. Because Patient 1 was found to be haploinsufficient for *APC*, he would be predicted to be at risk for developing adenomatous colonic polyps.

Our group previously reported the case of a 6-year-old boy with a 46,XY,del(10)(q23.2q23.33) karyotype who had dysmorphic facies, developmental delay, rectal bleeding from age 2 years, and multiple polyps extending from his duodenum to his rectum.[7] Biopsy showed classic juvenile polyps, with no evidence of dysplasia. Other family members reportedly had no intestinal polyps or any of the other physical findings of the patient. Molecular analysis of this individual's deletion showed it to be approximately 6.5 Mb in length, and to span the *PTEN* region (Fig. 2). The deletion in Patient 3 and the deletion in this boy appeared to have in common the loss of band 10q23.2. For that reason, we were particularly interested in comparing these two deletions. Again, while the deletion in patient three was localized immediately proximal to the *PTEN* region, it did not include this gene. Therefore, these two deletions which, by high-resolution chromosome analysis, both appeared to include band 10q23.2, were separated by < 1 Mb, a physical distance below the lower limits of microscopic resolution.

ATR-16, a syndrome associated with a chromosome 16 microdeletion of the α-globin locus, is characterized by α-thalassemia, mild to moderate mental retardation, and a broad spectrum of dysmorphology. Because of the subtlety of its corresponding cytogenetic findings and the mildness and variability of the phenotype, this syndrome is thought to be underdiagnosed.[22] With a physical length of approximately 7 Mb, the 16p deletion in Patient 3 included and extended beyond the 1 to 2 Mb critical region defined for this syndrome. Important in this patient is the fact that her deletion does not include other genes for which the phenotypic consequences of haploinsufficiency are significant, *PKD1*, *TSC2*, and that for Rubinstein-Taybi syndrome.

The fact that FISH and microsatellite studies can be systematically used to confirm and better characterize chromosomal aberrations is well known. But now these studies can, and should, be extended to show whether specific genes are, or are

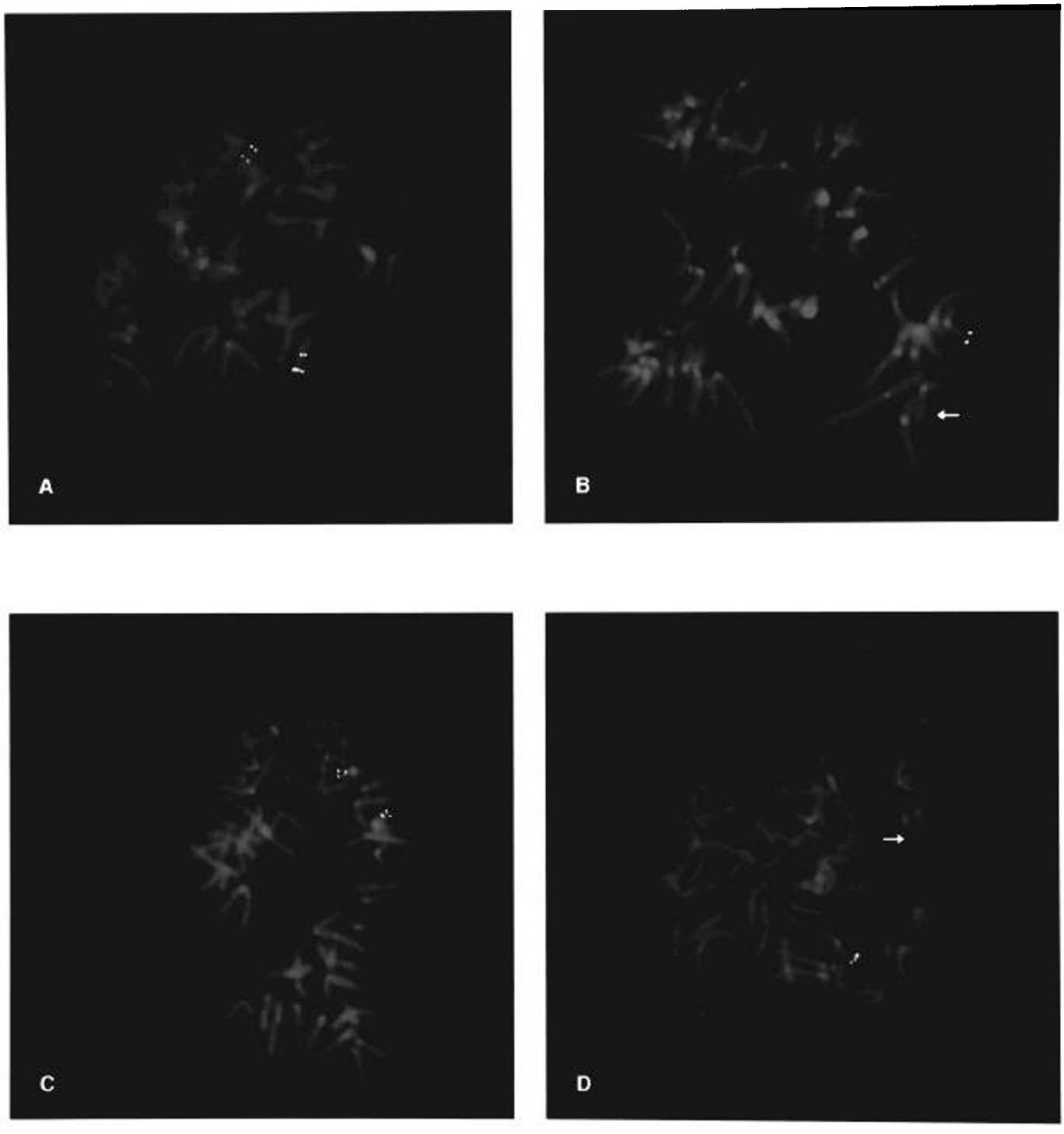

Fig. 3 Representative FISH with YAC clones. (A) Hybridization with the YAC clone 738B12, in the *PTEN* region, demonstrated signals on both chromosome 10 homologues in Patient 3. Two signals are seen, due to the chimeric nature of the clone. (B) A proximally located YAC clone, 898C3, displayed a signal only on the normal chromosome 10 homologue, which was absent from the deleted homologue, as indicated by the arrow. (C) In Patient 4, hybridization with the P1 clone 3699, in the *TSC2* region, demonstrates signals on both chromosome 16 homologues. Two signals are seen, due to the chimeric nature of the clone. (D) A positive hybridization signal for the YAC clone 650A8, which maps to the terminus of chromosome 16p, can be seen on the normal chromosome 16 but is deleted form the abnormal homologue, as indicated by the arrow.

not, deleted. This practice can allow for more precise phenotype-genotype correlations to be made in cases involving genes known to have an effect when haploinsufficient. The ability to make meaningful predictions of this nature will only improve as the body of physical mapping data available in the human genome databases becomes increasingly more complete, and as genes that are known to have a phenotypic effect when haploinsufficient are localized with greater accuracy.

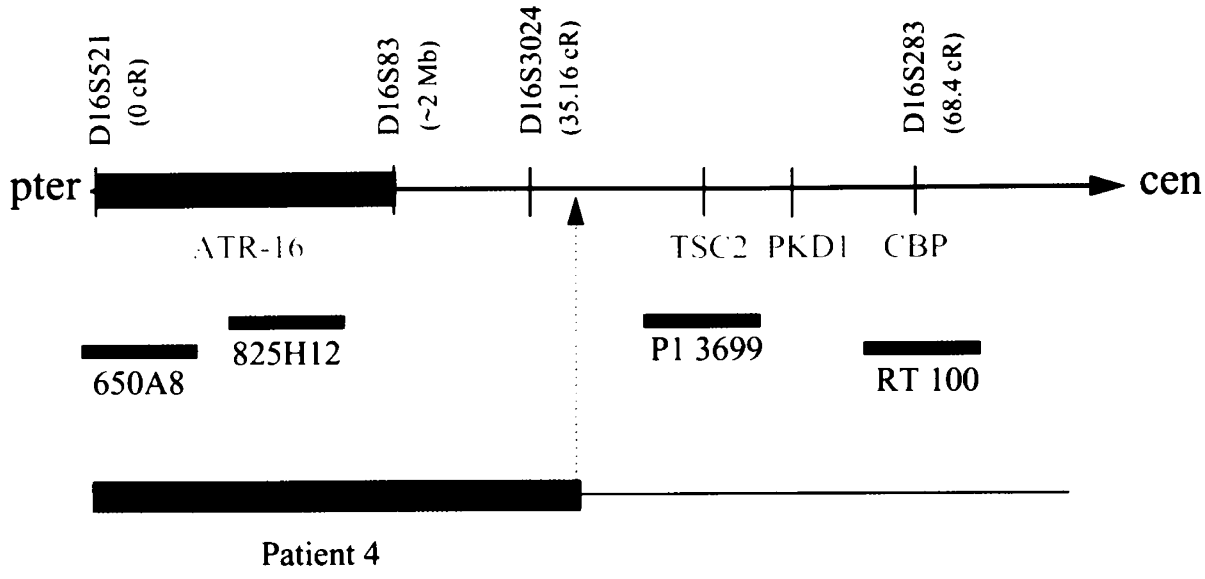

Fig. 4 Diagrammatic representation of chromosome 16p, not drawn to scale, denoting the deletion breakpoint in Patient 4. The short arm of chromosome 16 is depicted by the black arrow, and representative microsatellite markers, arrayed by physical location in centiRays (cR), are shown above. A black bar identifies the deleted region, with the approximate breakpoint indicated by the dotted line. Patient 4 demonstrates a deletion of approximately 7 Mb that includes the α-thalassemia-mental retardation critical region. The order of the markers and physical mapping information, in cR3000 units, are from the databases indicated in the text. For chromosome 16, the physical to genetic map correlate is 1 cR = 201 kb (Gyapay et al.).[15]

A potential caveat of these types of studies is the possibility of position effect, in that gene expression might be altered due to a change in the position of the gene relative to its normal chromosomal environment.[23] Given such a scenario, an individual in whom a deletion was localized at a distance from a specific gene might be deleted for *cis*-acting elements necessary for normal gene expression. Consequently, a gene that is ostensibly intact would not be properly expressed. Therefore, even in the presence of required regulatory elements, the chromosomal microenvironment imposed on a gene by a flanking deletion could inhibit these elements from functioning properly, resulting in malexpression of the gene.

Another caveat is the extent to which inconsistencies exist among the various physical mapping databases. Considerable time and effort is required to integrate and consolidate the best information currently available to create meaningful maps. Current information pertaining to the relative positions of genetic loci may prove to be imprecise in the future, as additional genomic data allow for further refinement of the physical maps. Therefore, it is advisable to update working maps regularly to reflect the best available genomic data.

Despite these caveats, molecular delineation of subtle chromosomal aberrations can provide results that assist in predicting clinical outcome and offer information for long-term clinical management. Therefore, we recommend that when a deletion or duplication is identified, the appropriate molecular analyses should be performed to ascertain the presence or absence of a specific testable gene or genes, localized to that region, that can have a phenotypic effect due to haploinsufficiency or excess gene dosage. Such studies can both assist in the prediction of clinical outcome for individual patients and lead to the recognition of significant associations between a particular phenotype and altered gene dosage at a particular locus.

Acknowledgment

The authors thank J. Marie Haren and Mary C. Karode at the Center for Human Genetics Laboratory for their expert technical assistance. This work was supported in part by funding from the Department of Human Genetics and the Center for Human Genetics at Case Western Reserve University and University Hospitals of Cleveland, a grant from the Wilson Foundation to the Center for Human Genetics, and by NIH grant PO1 HD 32,111 to S.S.

References

1. Franke U. Retinoblastoma and chromosome 13. *Cytogenet Cell Genet* 1976;14:131–134.
2. Stallard HB. The conservation treatment of retinoblastoma. *Trans Opthal Soc* 1962; 82:473.
3. Gey W. Dq-, multiple missbildungen und retinoblastom. *Humangenetik* 1970;10: 362–365.
4. Taylor AI. Dq-, Dr und retinoblastom. *Humangenetik* 1970;10:209–217.
5. Herrera L, Kakati S, Gibas L, Pietrzak E, Sandberg AA. Gardner syndrome in a man with an interstitial deletion of 5q. *Am J Med Genet* 1986;25:473–476.
6. Petrij F, Giles RH, Dauwerse HG, Saris JJ, Hennekam RCM, Masuno M, Tommerup N, van Ommen GJ, Goodman RH, Peters DJ, Breuning MH. Rubinstein-Taybi syndrome caused by mutations in the transcriptional co-activator CBP. *Nature* 1995;376:348–351.
7. Tsuchiya KD, Wiesner G, Cassidy SB, Limwongse C, Boyle JT, Schwartz S. Deletion 10q23.2-q23.33 in a patient with gastrointestinal juvenile polyposis and other features of a Cowden-like syndrome. *Genes Chromosomes Cancer* 1998;21:113–118.
8. Johns Hopkins University. The genome database, 1999. Available from: URL: http://www.gdb.org.
9. University of Southampton, Wessex Human Genetics Institute. Genetic Location Database, 1999. Available from: URL: http://cedar.genetics.soton.ac.uk/public_html/.
10. The National Center for Biotechnology Information (NCBI). UniGene human sequences collection, Gene Map 98, 1999. Available from: URL: http://www.ncbi.nlm.nih.gov/UniGene/Hs.Home.html.
11. Micale M, Haren JM, Conroy JM, Crowe CA, Schwartz S. Parental origin of de novo chromosome 9 deletions in del (9p) syndrome. *Am J Med Genet* 1995;57:79–81.
12. Pinkel D, Straume T, Gray JH. Cytogenetic analysis using quantitative, high-sensitivity, fluorescence hybridization. *Proc Natl Acad Sci USA* 1986;83:2934–2938.

13. Sullivan BA, Jenkins LS, Karson EM, Leana-Cox J, Schwartz S. Evidence for structural heterogeneity from molecular cytogenetic analysis of dicentric Robertsonian translocations. *Am J Hum Genet* 1996;59:167–175.
14. Whitehead Institute for Biomedical Research/MIT Center for Genome Research, Human Physical Mapping Project Database, 1998. Available from: URL: http://www.genome.wi.mit.edu.
15. Gyapay G, Schmitt K, Fizames C, Jones H, Vega-Czarny N, Spillett D, Muselet D, Prud'Homme JF, Dib C, Auffray C, Morissette J, Weissenbach J, Goodfellow PN. A radiation hybrid map of the human genome. *Hum Mol Genet* 1996;5:339–346.
16. Kobayashi T, Narahara K, Yokoyama Y, Ueyama S, Mohri O, Fujii T, Fujimoto M, Ohtsuki S, Tsuji K, Seino Y. Gardner syndrome in a boy with interstitial deletion of the long arm of chromosome 5. *Am J Med Genet* 1991;41:460–463.
17. Kinzler KW, Nilbert MC, Su L-K, Vogelstein B, Bryan TM, Levy DB, Smith KJ, Preisinger AC, Hedge P, McKechnie D, Finniear R, Markham A, Groffen J, Boguski MS, Altschul SF, Horii A, Ando H, Miyoshi Y, Miki Y, Nishisho I. Identification of FAP locus genes from chromosome 5q21. *Science* 1991;253:661–665.
18. Olschwang S, Laurent-Puig P, Melot T, Thuille B, Thomas G. High resolution genetic map of the adenomatous polyposis coli (APC) region. *Am J Med Genet* 1995; 56:413–419.
19. Nelen MR, Padberg GW, Peeters EAJ, Lin AY, van den Helm B, Frants RR, Coulon V, Goldstein AM, van Reen MM, Easton DF, Eeles RA, Hodgsen S, Mulvihill JJ, Murday VA, Tucker MA, Mariman EC, Starink TM, Ponder BA, Ropers HH, Kremer H, Longy M, Eng C. Localization of the gene for Cowden disease to chromosome 10q22–23. *Nature Genet* 1996;13:114–116.
20. The European Polycystic Kidney Disease Foundation. The polycystic kidney disease 1 gene encodes a 14 kb transcript and lies within a duplicated region on chromosome 16. *Cell* 1994;77:881–894.
21. Lamb J, Harris PC, Wilkie AOM, Wood WG, Dauwerse JHG, Higgs DR. De novo truncation of chromosome 16p and healing with (TTAGGG)n in the alpha-thalassemia/mental retardation syndrome (ATR-16). *Am J Hum Genet* 1993;52:668–676.
22. Lindor NM, Valdes MG, Wick M, Thibodeau SN, Jalal S. De novo 16p deletion: ATR-16 syndrome. *Am J Med Genet* 1997;72:451–454.
23. Kleinjan DJ; van Heyningen V. Position effect in human genetic disease. *Hum Mol Genet* 1998;7(10):1611–1618.